Jurnal Teknologi

Full Paper

IMPACT AND EVALUATION OF OPTIMIZED PV GENERATION IN THE DISTRIBUTION SYSTEM WITH VARYING LOAD DEMANDS

Hanis Farhah Jamahori[a], Md. Pauzi Abdullah[a]*, Abid Ali[b]

[a]Centre of Electrical Energy Systems, Institute of Future Energy, Universiti Teknologi Malaysia, 81310 Johor Bahru, Malaysia
[b]Interdisciplinary Institute of Technological Innovation (3IT), Université de Sherbrooke, 3000 Boulevard Université, Sherbrooke, J1K OA5 Québec, Canada

Article history
Received
31 May 2022
Received in revised form
11 February 2023
Accepted
17 February 2023
Published Online
19 April 2023

*Corresponding author
mdpauzi@utm.my

Abstract

Most distributed renewable energy generation (DREG) planning studies are performed using a constant load model and a dispatchable generation unit. However, the renewable generation unit and load demand vary in real life, and the generation size at the peak demand varies accordingly with loading levels. Such considerations may lead to the erroneous conclusion: the power loss reduction and bus voltage improvement may not be optimal. Consequently, the generation unit must be adequately integrated to offer optimal capacity in the distribution system while considering non-constant load demand as a part of DREG planning. Therefore, the impact of integrating photovoltaic (PV) considering historical solar weather data and varying load demand for five different voltage-dependent load models is proposed in this study. Particle swarm optimization (PSO) is employed to find the optimal location and size of PV with the objective to minimize power losses in the distribution system using IEEE 33-bus and IEEE 69-bus test systems. The findings are evaluated based on the comparative analysis of power losses reduction, PV penetration level, power loss index, and voltage deviation index. Findings revealed that the proposed model is effective in determining the optimal location and size of PV with a significant reduction of power losses that varies between 13.84% to 32.71% in 33-bus, and between 18.56% to 43.80% in 69-bus. In addition, the improvement in minimum bus voltage and other performance indices are also significant.

Keywords: Photovoltaic (PV), solar irradiance, time-varying load data, active and reactive power loss, voltage deviation

Abstrak

Kebanyakan kajian perancangan penjanaan tenaga boleh diperbaharui teragih (DREG) dilakukan menggunakan model beban malar dan unit penjanaan boleh dihantar. Walau bagaimanapun, unit penjanaan boleh diperbaharui dan permintaan beban berubah-ubah dalam kehidupan sebenar, dan saiz penjanaan pada permintaan puncak juga berubah mengikut tahap pemuatan. Pertimbangan sedemikian boleh membawa kepada kesimpulan yang salah: pengurangan kehilangan kuasa dan peningkatan voltan bas mungkin tidak optimum. Oleh itu, unit penjanaan mesti diintegrasi dengan tepat untuk memberi kapasiti yang optimum dalam sistem pengedaran untuk menampung permintaan beban yang tidak tetap sebagai sebagai sebahagian daripada perancangan DREG. Oleh itu, kesan mengintegrasi fotovoltan (PV) menggunakan hasil data sinaran suria dan permintaan beban yang berubah-ubah untuk lima model beban yang bergantung pada voltan berbeza dicadangkan dalam kajian ini. Pengoptimuman kawanan zarah (PSO) digunakan untuk menentukan lokasi dan saiz PV yang optimum dengan objektif untuk meminimumkan kehilangan kuasa dalam sistem pengedaran menggunakan sistem ujian IEEE 33-bas dan IEEE 69-bas. Penilaian dibuat berdasarkan analisis perbandingan pengurangan kehilangan kuasa, tahap penembusan PV, indeks kehilangan kuasa, dan indeks sisihan voltan. Keputusan menunjukkan bahawa model yang dicadangkan berkesan dalam menentukan lokasi dan saiz PV yang optimum dengan pengurangan ketara kehilangan kuasa yang berbeza antara 13.84% hingga 32.71% untuk 33-bas, dan antara 18.56% hingga 43.80% untuk 69-bas. Di samping itu, peningkatan dalam voltan bas minimum dan indeks prestasi lain juga meningkat.

Kata kunci: Fotovoltaik (PV)), sinaran suria, data beban yang berubah masa, kehilangan kuasa aktif dan reaktif, sisihan voltan

1.0 INTRODUCTION

Generally, the power delivery from the generation side to the consumer side through distribution networks is conveyed with high power losses due to Joule's effect accounting for 13% of the total generated energy in the electric network [1]. Methods for losses reductions that optimally improve the performance of the distribution network and to maintain the operating network at the highest efficiency level have gained much attention from utilities. The method includes the integration of distributed generation (DG), capacitor placement, and network reconfiguration. Among these, integration with DG is the most promising solution to this problem. DG is described as small-scale generating units positioned close to the served loads [2]. There are two categories of DG: renewable energy (RE) and non-renewable energy. The RE types are known as distributed renewable energy generation (DREG).

The rise in global energy consumption has made RE technologies more appealing in recent years. In addition to global warming and the rapid depletion of fossil fuel reserves, the use of RE has grown drastically during the last decade. Among all RE generation technologies currently available on the market, PV has received the most attention due to abundant solar availability in many countries, including Malaysia, and its affordable installation and maintenance costs. Furthermore, following the global expansion of the PV industry to use electrification for various applications, much research has been conducted on PV generation in the distribution system [3-7].

The study on DG planning considering PV types has been performed in [8-13] that discussed the impact of PV integration on the distribution system aimed to reduce losses and improve voltage profile. The result revealed that the integration of PV had shown promising results in reducing total losses and improving the voltage profile. However, most studies assumed PV as a dispatchable generation unit and ignored the fact that PV is a renewable energy type, where power output is greatly influenced by solar irradiation and geographical climate factors. In addition, only constant load data are considered to perform the DG planning analysis, which could further lead to getting of inaccurate results.

To ensure the PV works as a reliable and efficient system at a particular area, it is crucial to analyze the load profile of that area, as the lload profile will impact on the sizing and modeling of the generation unit. In addition, peak times in a load profile and customer behaviour affect the system's dependability on the generation size and allocation planning. The impact of PV penetration is also important aspect in DG planning, and only a few studies have done on this impact on time-varying loads. However, it is known that the penetration level varies with load demand. Therefore, it is crucial to consider both time-varying load and weather data in DREG planning to gain optimal PV integration.

The primary objective is to analyze the impact of PV considering non-constant load models to reduce power losses and voltage deviations in the distribution system. The study uses both time-varying weather and load data. The analysis is evaluated based on the comparative result of total active and reactive power losses, PV penetration level, and impact indices for different load models. 13-years of Malaysia's historical irradiance data from 2007 to 2020 is used based on a global solar radiation tracking system [14]. A beta distribution function is applied to estimate the hourly expected PV power output, and the PV size and location are optimized using Particle Swarm Optimization (PSO) based on the hourly expected PV power generated. The results are evaluated based on the comparative analysis of total PV penetration and size, total power losses, voltage deviation, and loss indices on constant, industrial, residential, commercial, and mixed load models.

2.0 METHODOLOGY

The modeling of system parameters, including formulations for load flow studies, test distribution system, modeling of PV using time-varying weather data, modeling of load model data, impact indices, and constraints applied in this study are provided in the sub-section.

2.1 Power Flow Analysis

The first step is to perform the power flow to find the base case values before PV integration in the distribution system. For this study, the system's power flow and base power loss are calculated using the Forward/Backward sweep-based numerical approach, which is proven more efficient and accurate than the other conventional methods [15, 16]. The branch's active power loss, $P_{loss\,(i,j)}$ and the respective reactive loss, $Q_{loss(i,j)}$ between two buses, i,j are calculated using the following expression [17]:

$$P_{loss(i,j)} = R_{ij}\left(\frac{P_i^2 + Q_i^2}{|V_i|^2}\right) \quad (1)$$

$$Q_{loss(i,j)} = X_{ij}\left(\frac{P_i^2 + Q_i^2}{|V_i|^2}\right) \quad (2)$$

where R_{ij} and X_{ij} represents the branch resistance and reactance between two buses, i, j and N_{bus} as the maximum bus in the system. The total power loss at I bus are the summation of the branch losses (3) and (4) given by [17]:

$$TP_{loss} = \sum_{i=1}^{N_{bus}} (P_{loss(i,j)} + jQ_{loss(i,j)}) \quad (3)$$

2.2 Load Profile

The load demand profile is calculated by multiplying an average daily load with the standard Radial

Distribution System (RDS) baseload, where the average daily load is calculated as a percentage of the peak hourly load. Consequently, these load models are technically referred to as time-varying voltage-dependent loads. The new load demand at bus i, which integrates time-varying loads at a specific period (t), is expressed using the following equations [18]:

$$P_{Dnew,i}(t) = P_{Di}(t)\ x\ V_i^{vp}(t) \quad (4)$$

$$Q_{Dnew,i}(t) = Q_{Di}(t)\ x\ V_i^{vq}(t) \quad (5)$$

where P_{Di}, and $P_{Dnew,i}$ are the actual and new active power load, respectively, Q_{Di}, and $Q_{Dnew,i}$ are the actual and new reactive power load, respectively, and V_i is the actual voltage magnitude at i bus calculated from the base caseload condition.

Figure 1 illustrates the normalized load demand curves for industrial, residential, and commercial customers. The value of both the active load voltage opponent, vp, and the reactive load voltage opponent, vq, are provided in Table 1 [18]:

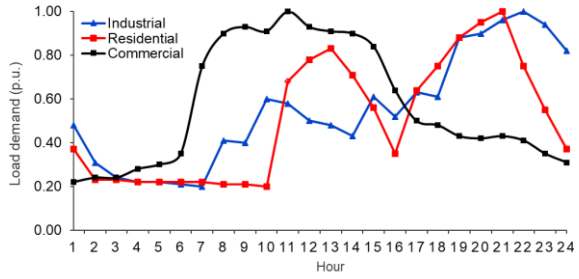

Figure 1 The normalized hourly load profile for varying load users

Table 1 Load model and its voltage coefficient

Load Types	vp	vq
Constant	0	0
Industrial	0.18	6.00
Residential	0.92	4.04
Commercial	1.51	3.40

This study considered both constant and different time-varying loads; industrial, residential, commercial, and mixed loads. Mixed load types are modeled by combining industrial, residential, and commercial user patterns according to voltage-dependent exponents defined in Table 1. The single line diagram for both systems is depicted in Figures 2 and 3.

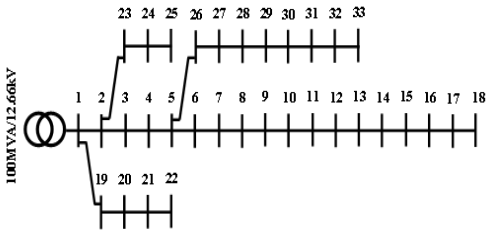

Figure 2 IEEE 33-bus system single-line diagram

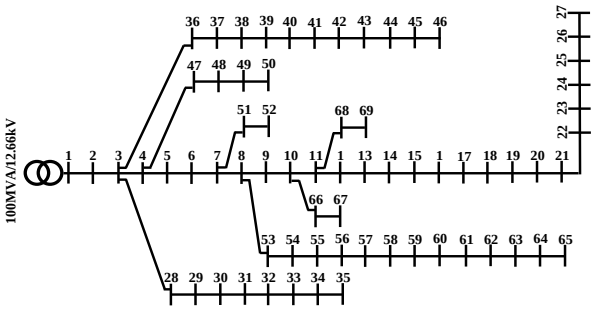

Figure 3 IEEE 69-bus system single-line diagram

2.3 PV Irradiance Modeling

The PV performance is influenced by the amount and intensity of solar irradiation at a particular site, temperature, and the characteristics of the PV module. In this study, the probability of the Beta-function is employed to predict the random occurrence of solar PV and model the solar irradiance at each interval. The mean, μ, and standard deviation, σ, are derived using thirteen years of solar irradiance data. The expression is given as [19]:

$$Beta(s) = \begin{cases} \dfrac{\Gamma(\alpha+\beta)}{\Gamma(\alpha)\Gamma(\beta)},\ s^{(\alpha-1)}(1-s)^{(\beta-1)}, \\ 0 \\ 0 \le s \le 1, \alpha, \beta \ge 0 \end{cases} \quad (6)$$

where s is a random variable of solar radiation (kW/m^2), values for a and β at each hour daily are generated using thirteen years of hourly historical solar irradiance data derived from μ and σ as provided in Table 2 are expressed using the following expressions [19]:

$$\alpha = \frac{\mu\beta}{(1+\mu)}\ ;\ \beta = (1-\mu)\left(\frac{\mu(1+\mu)}{\sigma^2} - 1\right) \quad (7)$$

The probability of solar irradiance, p(s) with irradiance limits of s1 and s2, is computed using the following formula [19]:

$$p(s) = \int_{s2}^{s1} Beta(s)\, ds \quad (8)$$

Table 2 Mean, μ and standard deviation, σ for 13 years averaged irradiance data, (kW/m^2)

Hour	μ	σ	Hour	μ	σ
7	0.001	0.001	14	0.697	0.206
8	0.038	0.019	15	0.609	0.206
9	0.173	0.066	16	0.473	0.194
10	0.358	0.119	17	0.305	0.159
11	0.539	0.155	18	0.149	0.097
12	0.665	0.181	19	0.045	0.033
13	0.712	0.196	20	0.005	0.005

2.4 Hourly PV Modeling

PV power is highly affected by weather conditions, temperature and solar irradiation. The PV output, PV_{NET} at respective solar irradiance s is calculated using [20]:

$$PV_{NET} = N\ x\ FF\ x\ V_{NET}\ x\ I_{NET} \quad (9)$$

$$FF = \frac{V_{MPPT}\ x\ I_{MPPT}}{V_{OC}\ x\ I_{SC}} \quad (10)$$

$$V_{NET} = V_{OC} - K_V\ x\ T_C \quad (11)$$

$$I_{NET} = s\left[\begin{matrix} I_{SC} + K_i \\ x\ (T_C - 25) \end{matrix}\right] \quad (12)$$

$$T_C = T_A + s\left(\frac{N_{OT} - 20}{0.8}\right) \quad (13)$$

where the main parameters of this equations are short circuit current, I_{SC} and open voltage circuit, V_{OC} , which is highly affected by the solar irradiance s. Other important parameters are the maximum voltage and current tracking point, V_{MPPT} , I_{MPPT} respectively and the fill factor, FF. N is the number of the module while N_{OT} is a nominal operating module, and T_C , T_A are the nominal cell and ambient temperature, respectively. Taking all these parameters into consideration, the total predicted PV output power at a particular hour, $PV_{out}(h)$ at $(h = 1\ \text{hour})$ can be expressed as follows [20]:

$$PV_{out}(h) = \int_0^1 PV_{NET}(s)\ p(s)\ ds \quad (14)$$

2.5 PV Integration

After integrating PV into the system, the new power load demand at i bus is determined as [20]:

$$P_{Dnew,i} = P_{PVi} - P_{Di} \quad (15)$$

$$Q_{Dnew,i} = Q_{PVi} - Q_{Di} \quad (16)$$

and

$$Q_i = a\ P_{PV\,i} - Q_{Di} \quad (17)$$

$$a = \pm\ tan(cos^{-1}(pf(P_i)) \quad (18)$$

where Q_i is the reactive PV power at i bus, pf is a power factor of the PV itself when is operating, a is positive (+) when PV generates reactive power; otherwise, it is negative (-). Since PV is known to generate only active power, it is assumed that the inverter works at a unity power factor.

Similarly, the new power losses after PV integration are calculated as [20]:

$$P^{PV}_{loss(i,j)} = R_{ij}\left(\frac{(P_{Di} - P_{PVi})^2 + (Q_{Di} - Q_{PVi})^2}{|V_i|^2}\right) \quad (19)$$

$$Q^{PV}_{loss(i,j)} = X_{ij}\left(\frac{(P_{Di} - P_{PVi})^2 + (Q_{Di} - Q_{PVi})^2}{|V_i|^2}\right) \quad (20)$$

Hence, the overall total losses in the system are given as [20]:

$$TP^{PV}_{loss} = \sum_{i=1}^{N_{bus}} (P^{PV}_{loss(i,j)} + jQ^{PV}_{loss(i,j)}) \quad (21)$$

2.6 Impact Index

Three impact indices are used to analyze the impacts of photovoltaic (PV) on both bus systems considering the time-varying load model and PV generation, are explained in the following sub-section.

2.6.1 Active and Reactive Power Loss Index (PLI, QLI)

The PLI is calculated as the final active output power ratio to the original base value, namely active power losses after PV integration to the active base case power losses without PV. Similarly, the QLI is calculated as the final reactive power losses ratio to original reactive losses without PV. Finally, both equations are expressed using [21]:

$$PLI = \frac{\sum_{h=1}^{24} PL_{PV}(h)}{\sum_{h=1}^{24} PL_{base\ case}(h)} \quad (22)$$

$$QLI = \frac{\sum_{h=1}^{24} QL_{PV}(h)}{\sum_{h=1}^{24} PL_{base\ case}(h)} \quad (23)$$

2.6.2 Voltage Deviation Index (VDI)

The VDI determines how much the present voltage magnitude deviated from its nominal value, V_{nom}. The ideal improved system should be zero. Hence, the voltage deviation between bus 1 and the maximum bus number in the system should be minimum and thus resulting in an improved voltage profile of the distribution network after PV is integrated, V_{PV}. The VDI is expressed using [21]:

$$VDI = max_{i=1}^{N_{bus}}\left(\frac{|V_{nom}| - |V_{PV}|}{|V_{nom}|}\right) \quad (24)$$

2.6.3 PV Penetration Level

The penetration level is calculated as the percentage of total PV output to the total demand consumption [21]:

$$PV\ Penetration, \% = \frac{\sum_{h=1}^{24} PV_{out}(h)}{\sum_{h=1}^{24} P_{Di}(h)}\ x\ 100 \quad (25)$$

2.7 Problem Formulation

The computational method is done based on minimizing the objective function subject to several constraints. The optimization used to locate and size the PV is briefly explained in this section.

2.7.1 Objective Function

The objective is to reduce system power losses; hence the problem can be stated as follows:

$$\min f = \sum_{h=1}^{24} \frac{TP_{Loss}\, PV}{TP_{Loss}\, basecase} \tag{26}$$

2.7.2 Power Balance Constraints

The objective function is subject to the following constraints follows [21]:

$$P_{ss} + PV_{out}(h) = P_{Dnew,i}(t) + P_{loss,i}(t) \tag{27}$$

$$Q_{ss} + QV_{out}(h) = Q_{Dnew,i}(t) + Q_{loss,i}(t) \tag{28}$$

where P_{ss}.and Q_{ss} are substation active and reactive power supplies to the distribution system. Therefore, the generated total power equals the total load demand and losses in the distribution network.

2.7.3 Bus Voltage Constraints

To preserve power quality, voltage magnitude at each bus must be within their permitted limit. Therefore, a maximum bus voltage magnitude is set at V_{nom}1.0 p.u [21]:

$$V_{i\,min} \leq V_i \leq V_{i\,max} \tag{29}$$

2.8 Optimization Formulation

2.8.1 Particle Swarm Optimization

PSO is a population-based stochastic optimization method that Dr. Kennedy and Dr. Eberhart developed in 1995 to optimize for a large number of combination problems [7]. The PSO concept is inspired based on the social behaviour of animals, such as fish schooling and birds flocking, which guide the particles in their exploration to find their global optimal solutions. PSO is an iterative algorithm, and each particle has its own velocity and position. All particles travel in a multidimensional search space to find the local and global optimal solution by locating the entire high-dimensional problem space [22, 23]. The basic principle underlying PSO is to use a random weighted acceleration at each time step to accelerate each particle toward its personal best, $pbest$ and global best, $gbest$ location. Each particle attempts to change its position by solving the following equation [24]:

$$v_i^{k+1} = wv_i^k + c_1 r_1 (pbest_i - s_i^k) + c_2 r_2 (gbest - s^k) \tag{30}$$

$$s_i^{k+1} = s_i^k + v_i^{k+1} \tag{31}$$

where v_i is the initial velocity of a particle i at iteration k, w is the weighting function, c_1 and c_2 are the weighting factor, usually is equal to 2, r_1 and r_2 are the random number between 0 and 10, v_i^{k+1} is the modified velocity of particle iteration i, s_i^k is the current position of a particle i at iteration k, and s_i^{k+1} is the modified position of a particle i. The flowchart of PSO is shown in Figure 4.

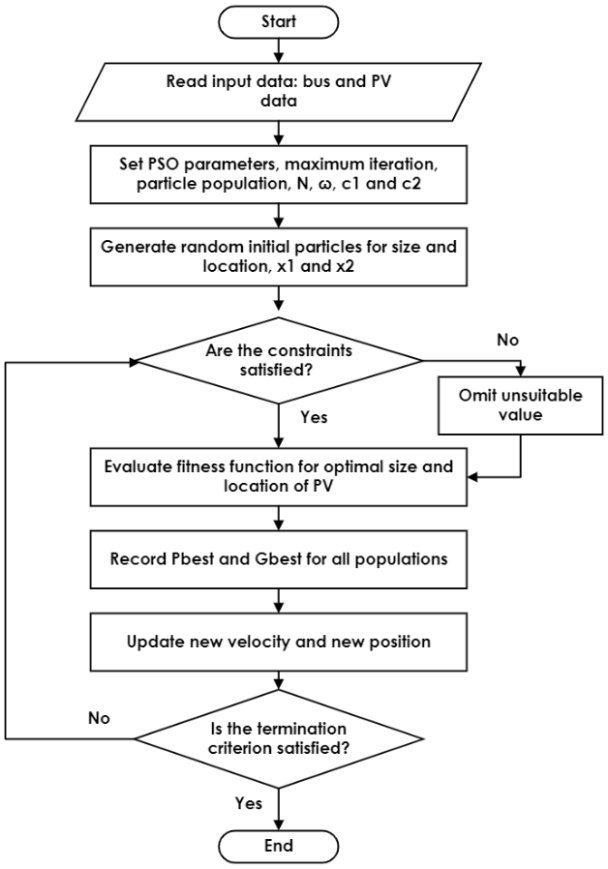

Figure 4 Flowchart of PSO process

The algorithm of the PSO is as follows. First, it is initialized the input bus data, PV data, and PSO settings, including the initialization of the input population. Then the power flow is examined in the bus test system to calculate the initial result of power loss and voltage magnitude without PV placement. The optimal location is determined by the weakest bus found after a load flow simulation. Next, the PSO algorithm is applied to determine the best location and size of PV. PSO will start with a group of random particles and then finds optima by updating generations. Finally, it will calculate total power loss and voltage magnitude by placing PV on every bus. If the power loss and voltage deviation are found at a minimum value, that location will be selected as the current best location. The iteration is repeated until the best location where power loss and voltage regulation are at a minimum is found. Each iteration of the PSO will evaluate the load flow to ensure that the equality and inequality constraints specified before are satisfied and that the optimal solution is attained.

The sizing and placement of PV on the system are subject to these constraints:

$$2 \leq PV_{location} \leq N_{bus} \quad (32)$$

The PV unit can be placed anywhere up to the maximum number of buses in the system, N_{bus} except of bus number 1 as it is considered as slack bus in the distribution system.

$$0 \leq PV_{size} \leq \sum_{i=1}^{N_{bus}} P_{Di} \quad (33)$$

The PV unit can only work within the permissible size range. As a result, the size should be designed in accordance with the load size. To avoid exceeding the entire load demand at i bus, the total generation size must be between zero and maximum load demand.

3.0 RESULTS AND DISCUSSION

The findings of the PV integrations performance and its impacts on the time-varying load model are discussed accordingly. The optimization is implemented on the standard distribution system, IEEE-33 bus, and IEEE-69 bus while considering different non-constant load models. The power loss and voltage magnitude before and after PV integration are determined using load flow analysis. Then, these results are used to calculate loss impact indices, voltage deviation indices, and PV penetration levels for different load models.

3.1 Simulation Results

Tables 3 and 4 shows the simulation results for the optimal DREG sizes and locations for each load cases in both buses. It is known that the optimal bus location for the 33-bus is at bus 6. Therefore, the optimal PV sizes are 2.60 MW, 1.81 MW, 2.08 MW, 2.85 MW, and 2.04 MW, respectively, while the optimal bus location for the 69-bus system is bus 61. Therefore, the corresponding installed PV sizes are 1.68 MW, 1.33 MW, 1.52 MW, 2.09 MW, and 1.35 MW, respectively, for constant, industrial, residential, commercial, and mixed loads. The remaining parameters are discussed in the next section.

3.2 Hourly Expected PV Output

Figure 5 depicts the average daily solar irradiation. The solar output is calculated using (14) for solar production in one day based on thirteen years of average data (07:00 to 20:00). The PV output is calculated using data gathered from the mentioned site. The daily expected PV output produced follows the normalized expected PV curve. The hourly estimated PV production for each load model is determined based on the average solar PV data.

Table 3 Simulation result of the IEEE-33 bus system performance parameters for each load model

Parameters/Load Model	Constant	Industrial	Residential	Commercial	Mixed
PV Location @ Size (MW)	6 @ 2.60	6 @ 1.81	6 @ 2.08	6 @ 2.85	6 @ 2.04
P_{loss} without PV (kW)	5063.96	1772.43	1606.40	1952.14	1644.16
P_{loss} with PV (kW)	4164.13	1527.18	1273.82	1313.54	1325.01
P_{loss} reduction, %	17.77	13.84	20.70	32.71	19.41
Q_{loss} without PV (kVAR)	3432.79	1200.67	1088.19	1322.56	1118.87
Q_{loss} with PV (kVAR)	2875.25	1051.63	885.48	931.81	927.94
Q_{loss} reduction, %	16.24	12.41	18.63	29.54	17.06
V_{min} (p.u)	0.9087	0.9224	0.9663	0.9719	0.9462
Weakest Bus	18	18	18	18	18
PV Penetration, %	20.82	26.47	33.10	40.15	30.40

Table 4 Simulation result of the IEEE-69 bus system performance parameters for each load model

Parameters/Load Model	Constant	Industrial	Residential	Commercial	Mixed
PV Location @ Size (MW)	61 @ 1.68	61 @ 1.33	61 @ 1.52	61 @ 2.09	61 @ 1.35
P_{loss} without PV (kW)	5398.74	1882.12	1705.66	2074.32	1832.34
P_{loss} with PV (kW)	4169.81	1532.81	1231.99	1165.83	1474.17
P_{loss} reduction, %	22.76	18.56	27.77	43.80	19.55
Q_{loss} without PV (kVAR)	2451.39	856.69	776.41	943.79	828.67
Q_{loss} with PV (kVAR)	1923.50	704.60	570.16	548.60	671.69
Q_{loss} reduction, %	21.53	17.75	26.56	41.87	18.94
V_{min} (p.u)	0.9198	0.9268	0.9683	0.9736	0.9306
Weakest Bus	27	27	27	27	27
PV Penetration, %	13.21	19.00	23.54	28.72	20.02

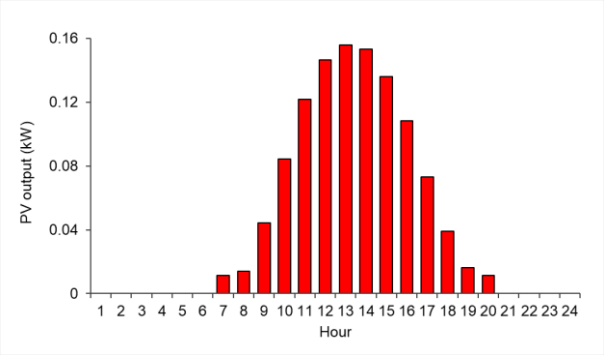

Figure 5 Average thirteen-years PV output power in Malaysia

Figures 6(a)–(b) depict the hourly estimated PV production for the optimum bus for each load model on both buses. Based on the figures, it can be seen that both buses exhibit a similar expected curve output. However, the PV output is greater with varying load models in the 33-bus than in the 69-bus.

3.3 PV Generation and Demand Consumption

Figures 7 and 8 demonstrate the hourly PV output and system demand for 33-bus and 69-bus test systems, respectively. For both bus systems, the size of PV units is larger with commercial load demand than residential and industrial loads.

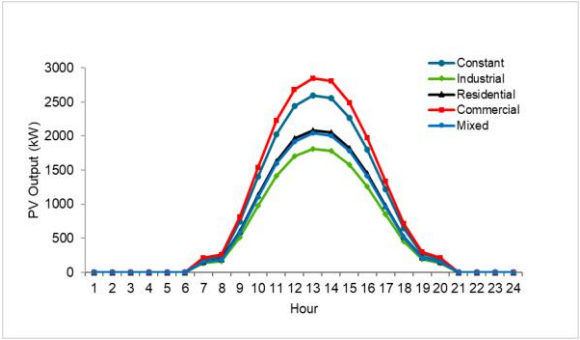

(a)

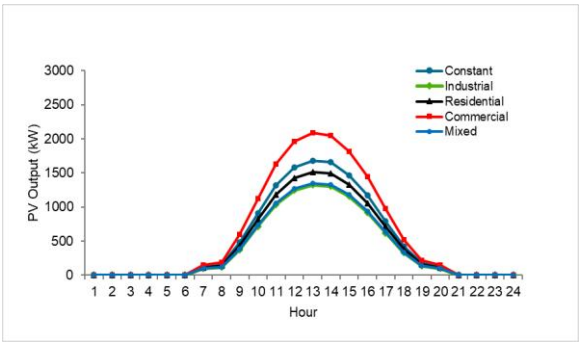

(b)

Figure 6 The expected PV output at optimal bus 6 and 61 at (a) 33-bus system and (b) 69-bus system for each load model

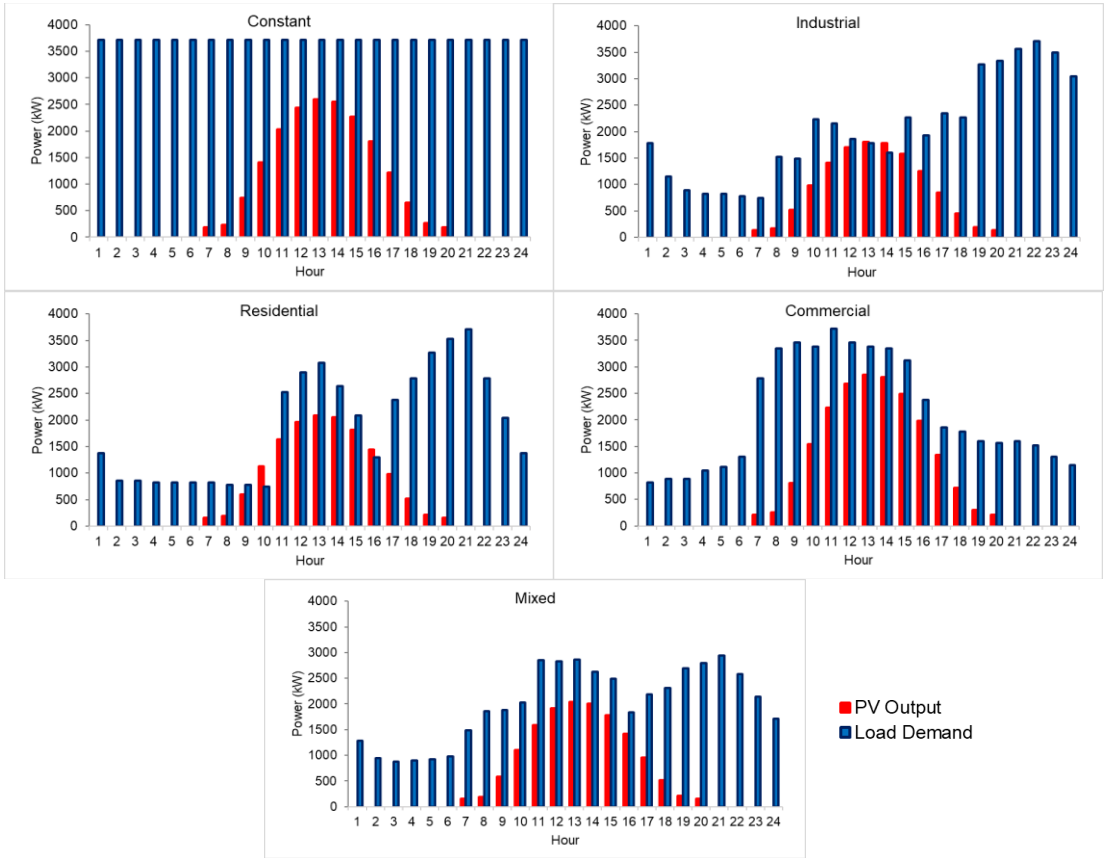

Figure 7 The hourly expected PV power generated and load demand consumption of the 33-bus system

Generally, this is due to commercial load consumption, and solar PV production is more matches throughout the day; low in the night to morning hours but peaks in noon hours. In contrast, the remaining load consumption is highest at night when solar PV production is unavailable. As a result, the maximum PV size is largest for commercial- and lowest for industrial. In addition, the output curve for the mixed load model is almost comparable to residential and industrial load, where PV size for the mixed load is slightly 1.92% and 1.48% bigger than that of residential and industrial load for 33-bus and 69-bus, respectively. It is revealed that PV generates larger power output when dealing with 33-bus load demand than 69-bus load demand. The generation size is more significant with commercial load demand than with constant, residential, and industrial loads for both bus systems. The PV output for mixed load is similar to residential in 33-bus, and similar to industrial in the 69-bus system.

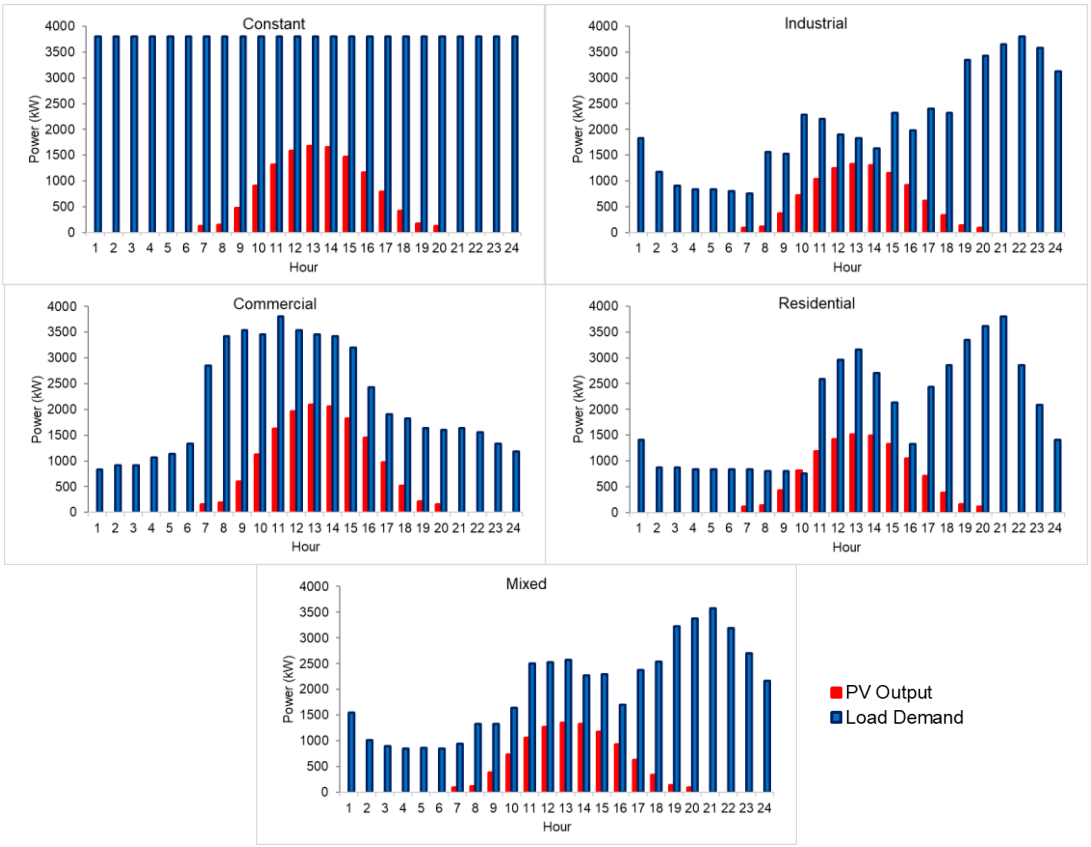

Figure 8 The hourly expected PV power generated and load demand consumption of the 69-bus system

3.4 Power Losses Reduction

The impact of PV to reduce losses in the system after the optimal size and location of PV were obtained using PSO method is presented and discussed. Also, the result of total power losses with and without PV are compared to evaluate its performance in the distribution system. Figures 9 and 10 depict the results of hourly power losses for each load model with and without PV placement in both bus systems. In corresponding with the PV size, the commercial load model has the most significant power loss reduction with 32.71%, residential with 20.70%, and mixed load with 19.41%. In contrast, the industrial load has the lowest power loss reduction at only 13.84%. The lowest loss reduction happens when the PV generation-cannot fulfill the load demand that experiences peak consumption at night, especially for the industrial and residential load. Also, an excess PV output is produced, which both industrial and residential load models did not consume at noon. Even though the PV production matches the mixed load model from morning to noon, PV output cannot meet the high load demand consumption at night. In contrast, the PV production and demand consumption for commercial demand matched better throughout the day, resulting in the highest power loss reduction, especially during peak hours at 11:00. The losses of each load model from 21:00 until 06:00 remain the same as there was no PV production during that period.

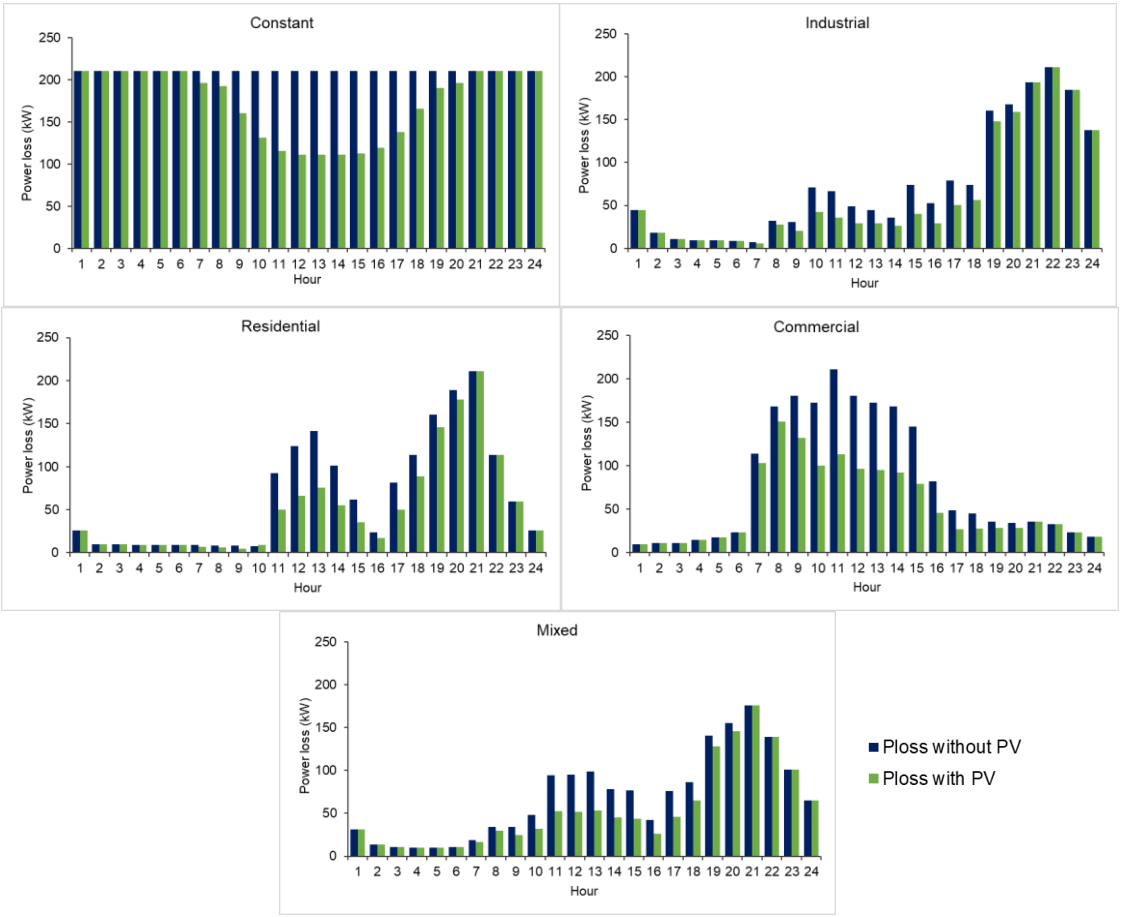

Figure 9 Hourly power losses for each load model with and without PV placement in 33-bus system

First, it can be observed from both results that different load cases have a different impact on the PV size. For the 33-bus system, the size of the PV is the smallest with industrial load compared to all load models. The active and reactive system loss has been slightly reduced by 13.84% and 12.41%, while the minimum voltage has improved to 0.9224 p.u from the base case value, 0.9038 p.u. In contrast, the size of the PV is the largest with a commercial load. Since PV production and load demand consumption are more match to commercial load, the active and reactive losses significantly reduced by 32.71% and 29.54%, respectively, while the minimum voltage has increased to 0.9719 p.u. The hourly expected PV generation for residential and mixed loads is almost similar for these two loads, as depicted in Figure 9. In corresponding to the PV size, the active and reactive system loss has reduced by 20.70% and 18.63% with residential load and 19.41% and 17.06% with mixed load, respectively. The minimum voltage has increased to 0.9663 p.u. and 0.9462 p.u., respectively, for the residential and mixed load.

Similar to the 33-bus system results, sizing for PV units is the lowest with industrial load and the largest with the commercial load for the 69-bus system. Active and reactive power losses decreased slightly with industrial load by 18.56% and 17.75%, respectively, but significantly with commercial load by 43.80% and 41.87%, respectively. As a result, the minimum voltage has improved from the base case value of 0.9092 p.u. to 0.9268 and 0.9736 p.u., respectively, for the industrial and commercial load. The mixed load model has almost similar hourly expected PV generation with industrial load consumption. The mixed load PV size is slightly larger than the industrial load PV size. Thus, the active and reactive losses for mixed load are 19.55% and 18.94%, respectively, with a minimum voltage of 0.9306 p.u. For residential load demand, integration of PV units has resulted in a 27.77% and 26.56% of active and reactive loss reduction, respectively. Accordingly, the minimum bus voltage improved to 0.9683 p.u.

The losses of each load model from 21:00 till 06:00 remain the same as there was no PV production during that period. For constant load demand, as the load consumption is constant throughout the day, the loss reduction only showed reduction following the PV production curve. The larger PV size for commercial load demand results in a significant loss reduction in both bus systems. In comparison, it is the lowest for industrial, implying a slight reduction in losses due to high demand consumption but no PV production at

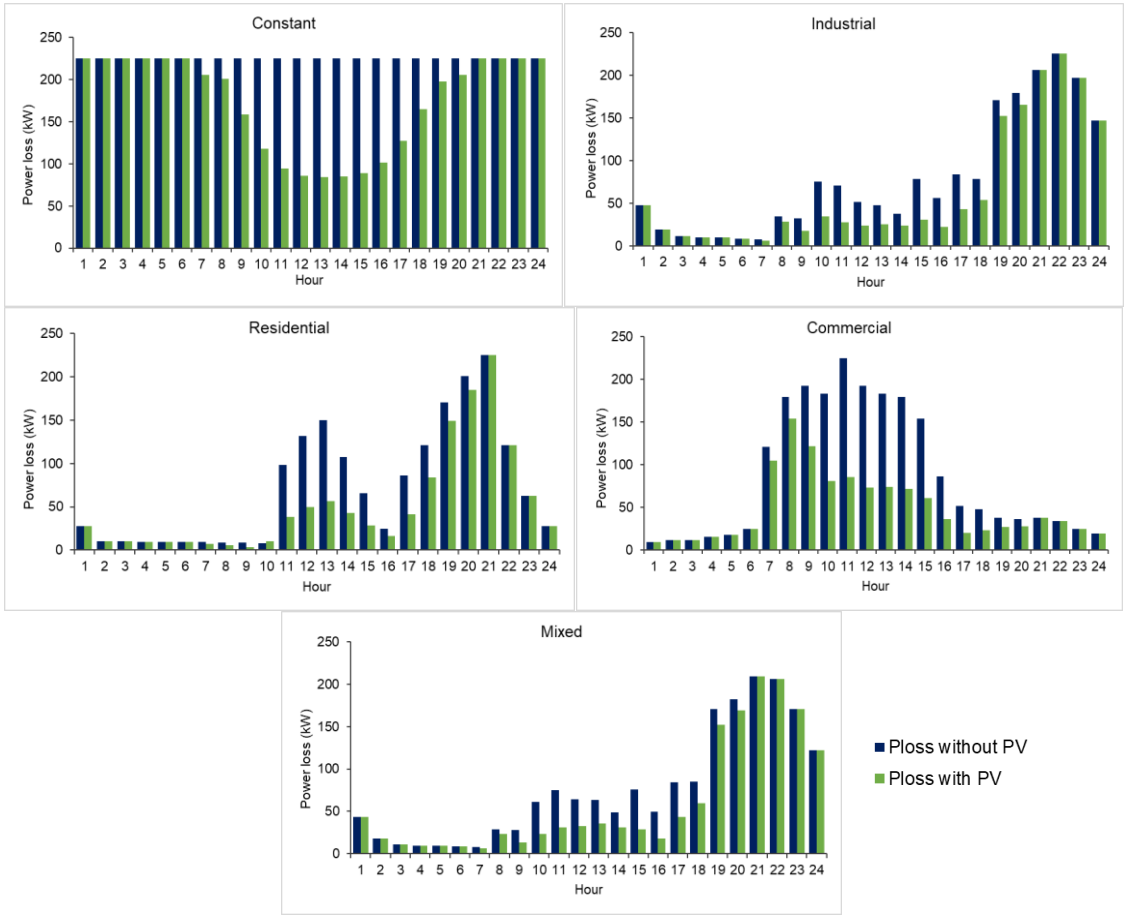

Figure10 Hourly power losses for each load model with and without PV placement in 69-bus system

night. In addition, PV size for mixed load demand is almost comparable to industrial load and residential load in 33-bus and 69-bus, respectively. This is because the power losses for these two load demands are almost similar. Hence, the residential and mixed loads exhibit similar load demand trends.

Accordingly, the mixed load is modelled as a combination of other types of load models (industrial, residential, and commercial) in both distribution systems. Therefore, it mimics the load pattern for these load models throughout the day. As the commercial has high power consumption at noon, the residential and industrial loads on the hand, have high power consumption at night. The unavailability of PV production at night affects the supply of power to the load. Therefore, the power loss reduction for any load that has high consumption at night (industrial, residential, and mixed load) is not significant during the period when the PV supply is lower and unavailable. The power loss in the electrical networks at any hour depends on the amount of loads connected at that particular time. The supply of electricity from PV modules during the daytime hours has resulted in reductions in net loads of the network, which also resulted in reduced power losses. However, during the late evening and night hours, the supply from PV modules became zero, the power losses with and without PV during these hours have remained unchanged.

Based on the results and figures presented, it is shown that PV integration into the distribution system has directly impacted the percentages of power loss reduction. The most significant reduction in power losses for both bus systems occurs when PV is integrated with commercial loads. In contrast, the most negligible reduction occurs when PV is integrated with industrial loads. Hence, it is important to evaluate a non-constant load model with PV integration as it provides more accurate results to deal with the real-time daily load consumers.

3.5 PV Penetration

PV penetration is one of the important impacts to consider when dealing with the integration of RE in DREG planning. A high penetration level indicates that the PV output generated is able to satisfy the load demand required on that particular day and vice-versa. Figure 11 shows the PV penetration level for all time-varying load models used in the 33-bus and 69-bus test systems. It depicts that different load models have different impacts on the PV penetration level. For the 33-bus system, the penetration levels are 20.82%, 26.47%, 33.10%, 40.15%, and 30.40%, respectively, for

the constant, industrial, residential, commercial, and mixed load. Similarly, for the 69-bus system, the penetration levels are 13.21%,19.00%, 23.54%, 28.72%, and 20.02%, respectively. It is known that the PV penetration level is higher with time-varying commercial load for both bus systems. As previously discussed, the commercial load consumption and solar PV production match more throughout the day than the other load. Furthermore, the imbalance between PV output and load demand consumption results in lower PV penetration levels, as seen in constant and industrial load demand.

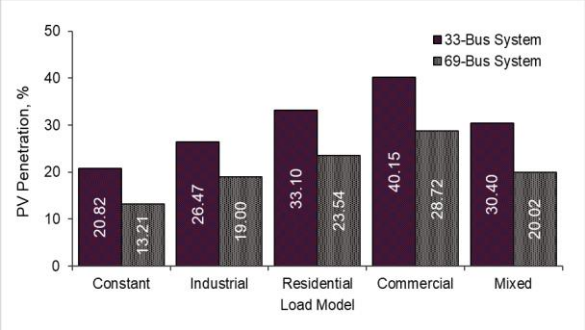

Figure 11 PV penetration level for all load models in 33-bus and 69-bus

3.6 Impact Indices

3.6.1 *Active and Reactive Loss Index (PLI, QLI)*

The PLI and QLI are calculated with and without PV integration into the distribution system, based on active and reactive power losses. The values of these impact indices for both test systems are plotted in Figures 12 (a) and (b). Based on the result, a high index of PLI and QLI indicates that PV integration has a negligible impact on reducing power losses. In contrast, a low index indicates a significant loss reduction to the power system.

The result shows that both indices exhibit a similar trend, with a better impact on 69-bus than 33-bus. Both indices are relatively low for commercial load but relatively high for industrial load demand. Hence, PV has a more significant impact on the commercial load and is almost negligible with industrial than the other load models. This is owing to the fact that PV generation and commercial load consumption occur concurrently during the day, whereas industrial, residential, and mixed load consumption occurs at night.

3.6.2 *Voltage Deviation Index (VDI)*

The reduction of power loss has a direct impact on the voltage profile of the distribution system. The highest power loss reduction will result in high voltage improvement and vice versa, thus resulting in the voltage deviation index at the lowest value. The bus with the lowest voltage is bus 18 for 33-bus systems and bus 27 for 69-bus systems, with minimum voltages of 0.9087, 0.9224, 0.9663, 0.9719, and 0.9462 and 0.9198, 0.9268, 0.9683, 0.9736, 0.9306 p.u. for constant, residential, commercial, and mixed loads in 33-bus and 69-bus respectively.

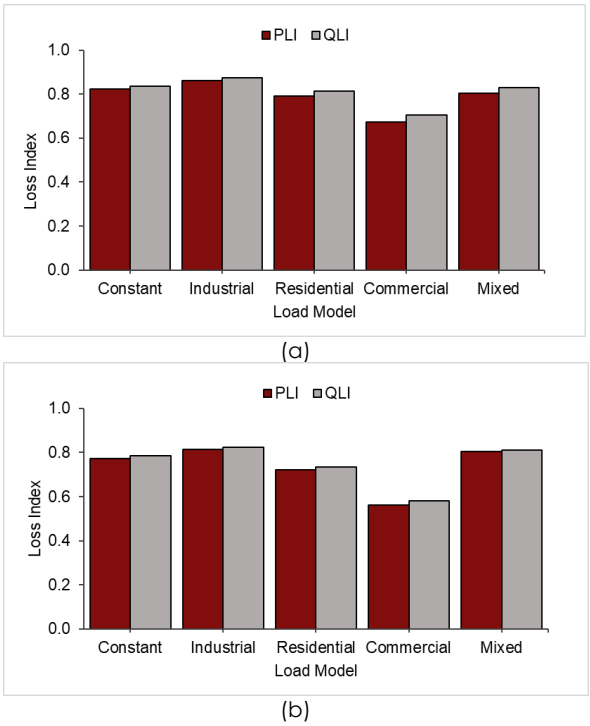

Figure 12 Loss impact index for (a) 33-bus system and (b) 69-bus system

The constant load model had the lowest voltage magnitude, which contributed to the high VDI value. In contrast, the commercial load model showed the most voltage improvement, resulting in the lowest VDI value.

The VDI of the ideal improved system performance should be zero or as small as possible so that the present voltage in the system does not deviate too much from its nominal value. The earlier simulation results show that the minimum voltage has improved for all load types compared to the constant baseload. The commercial load model showed the most significant voltage improvement, followed by residential, mixed, and industrial load demand.

Figure 13 depicts the VDI profile for each bus. The commercial load model has the lowest index and is closest to zero for the non-constant load model. In contrast, it is highest in industrial load, indicating more voltage has deviated from the original value.

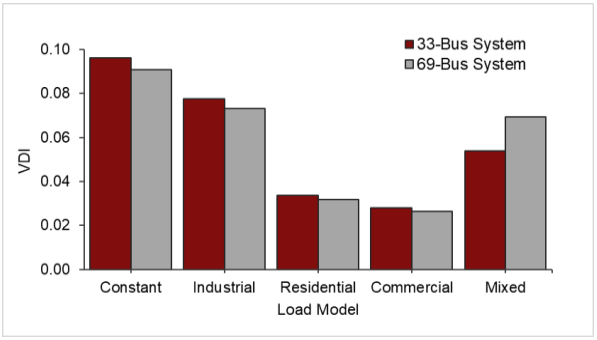

Figure 13 Voltage deviation index for 33-bus and 69-bus

4.0 CONCLUSION

In this study, the effectiveness of the PSO algorithm with the objective function of minimize total loss and voltage deviation using simultaneous time-varying load and solar irradiance data was tested on IEEE 33-bus and 69-bus test systems. The findings of this study are evaluated based on the comparative analysis done on total active and reactive power losses, PV penetration level, and different impact indices for different load models. The results revealed that PV integration has a different impact on non-constant load data.

First, the losses reduction was reduced by 13.84% - 32.71% for 33-bus, and 18.56%-43.80% for 69-bus, respectively. The reduction is highest for PV integrated with commercial load and the lowest for the industrial load. Second, the integration of PV has also shown a positive impact on the improvement of minimum voltage at peak hour load in both bus systems. There is a significant reduction in voltage deviation due to PV installations for all load types compared to the base values. Third, the PV size is largest for commercial demand and lowest for industrial demand. The optimal PV size ranged from 1.81MW to 2.85MW in 33-bus, and 1.33MW to 2.09MW in 69-bus system, both largest for commercial demand and the lowest for industrial demand.

Finally, the imbalance between the PV production and load demand consumption, particularly for the constant and industrial load models, led to a much lower PV penetration level, significant loss, and high voltage deviation. This is due to commercial load consumption matched with solar PV production throughout the day. Thus, PV would be a valuable addition to the network in areas with commercial loads, compared to constant and other non-constant load models.

Conflicts of Interest

The author(s) declare(s) that there is no conflict of interest regarding the publication of this paper.

Acknowledgment

The authors wish to thank the Ministry of Higher Education (MOHE) Malaysia and Universiti Teknologi Malaysia (UTM) for supporting the research under UTM Research University Grant (vote no: Q.J130000.3551.07G63).

References

[1] Yandri, E., 2017. The Effect of Joule Heating to Thermal Performance of Hybrid PVT Collector during Electricity Generation. *Renewable Energy*. 111.

[2] Chen, W.-M., *et al*. 2015. A Regional Energy Planning Approach: An Integrated Framework and Its Application to Jeju Island's Renewable Roadmap. Handbook of Research on Sustainable Development and Economics. K. D. Thomas, Editor. 2015, IGI Global: Hershey, PA, USA. 194-220.

[3] Arritt, R. F. and R. C. Dugan. 2011. Distribution System Analysis and the Future Smart Grid. *IEEE Transactions on Industry Applications*. 47(6): 2343-2350.

[4] Babacan, O., W. Torre, and J. Kleissl. 2017. Siting and Sizing of Distributed Energy Storage to Mitigate Voltage Impact by Solar PV in Distribution Systems. *Solar Energy*. 146: 199-208.

[5] Hemakumar Reddy, G., *et al*. 2019. Impact of Electric Vehicles on Distribution System Performance in the Presence of Solar *PV* Integration. *International Journal of Computational Intelligence & IoT*. 2(1).

[6] Hill, C. A., *et al*. 2012. Battery Energy Storage for Enabling Integration of Distributed Solar Power Generation. *IEEE Transactions on Smart Grid*. 3(2): 850-857.

[7] Jayavarma, A. and T. Joseph. 2013. Optimal Placement of Solar *PV* in Distribution System using Particle Swarm Optimization. *International Journal of Advanced Research in Electrical, Electronics and Instrumentation Engineering*. 2(1).

[8] Loji, K., I. E. Davidson, and R. Tiako. 2019. Voltage Profile and Power Losses Analysis on a Modified IEEE 9-Bus System with PV Penetration at the Distribution Ends. *2019 Southern African Universities Power Engineering Conference/Robotics and Mechatronics/Pattern Recognition Association of South Africa (SAUPEC/RobMech/PRASA)*. IEEE.

[9] Rajaram, R., K. S. Kumar, and N. Rajasekar. 2015. Power System Reconfiguration in a Radial Distribution Network for Reducing Losses and to Improve Voltage Profile using Modified Plant Growth Simulation Algorithm with Distributed Generation (DG). *Energy Reports*. 1: 116-122.

[10] Abujubbeh, M., M. Fahrioglu, and F. Al-Turjman. 2021. Power Loss Reduction and Voltage Enhancement via distributed Photovoltaic Generation: Case Study in North Cyprus. *Computers & Electrical Engineering*. 95: 107432.

[11] Hraiz, M. D., *et al*. 2020. Optimal PV Size and Location to Reduce Active Power Losses while Achieving Very High Penetration Level with Improvement in Voltage Profile using Modified Jaya Algorithm. *IEEE Journal of Photovoltaics*. 10(4): 1166-1174.

[12] Mohammadi, E. and S. Esmaeili. 2012. A Novel Optimal Placement Of PV System for Loss Reduction and voltage Profile Improvement. *International Journal on Technical and Physical Problems of Engineering (IJTPE)*. 4: 6.

[13] Marneni, A., A. Kulkarni, and T. Ananthapadmanabha. 2015. Loss Reduction and Voltage Profile Improvement in a Rural Distribution Feeder using Solar Photovoltaic Generation and Rural Distribution Feeder Optimization Using HOMER. *Procedia Technology*. 21: 507-513.

[14] Solcast. 2018. *Solar Irradiance Data*. [cited 2021. Available from: https://solcast.com/solar-radiation-data/.

[15] Eminoglu, U. and M. Hocaoglu. 2009. Distribution Systems Forward/Backward Sweep-based Power Flow Algorithms: A Review and Comparison Study. *Electric Power Components and Systems*. 37: 91-110.

[16] Issicaba, D. and J. Coelho. 2016. Evaluation of the Forward-Backward Sweep Load Flow Method using the Contraction

Mapping Principle. *International Journal of Electrical and Computer Engineering (IJECE)*. 6: 3229-3237.
[17] Chiradeja, P. 2005. *Benefit of Distributed Generation: A Line Loss Reduction Analysis*. 2005: 1-5.
[18] Hung, D., M. Nadarajah, and K. Lee. 2014. Determining PV Penetration for Distribution Systems With Time-Varying Load Models. *IEEE Transactions on Power Systems.*
[19] Atwa, Y. M., *et al*. 2010. Optimal Renewable Resources Mix for Distribution System Energy Loss Minimization. *IEEE Transactions on Power Systems.* 25(1): 360-370.
[20] Ali, A., *et al*. 2018. Sizing and Placement of Solar Photovoltaic Plants by using Time-series Historical Weather Data. *Journal of Renewable and Sustainable Energy*. 10(2): 023702.
[21] Ahmed, I. M., *et al*. 2018. Optimal Allocation of PV Based DG in Distribution Networks at Different Load Levels. *2018 Twentieth International Middle East Power Systems Conference (MEPCON)*.
[22] Kumari, R. L., *et al*. Optimal Sizing of Distributed Generation using Particle Swarm Optimization. *2017 International Conference on Intelligent Computing, Instrumentation and Control Technologies (ICICICT)*. 2017. IEEE.
[23] Bouktir, T. and K. Guerriche. 2015. Optimal Allocation and Sizing of Distributed Generation with Particle Swarm Optimization Algorithm for Loss Reduction. *Science and Technology*. 6(1): 59-69.
[24] Rani, B. J. and A. S. Reddy. 2019. Optimal Allocation and Sizing of Multiple DG in Radial Distribution System using Binary Particle Swarm Optimization. *International Journal of Intelligent Engineering and Systems.* 12(1): 290-299.